Mechanism for Ordered Receptor Binding by Human Prolactin†

Umasundari Sivaprasad,‡ Jeffrey M. Canfield,§,⊥ and Charles L. Brooks*,‡,§

The Ohio State Biochemistry Program and Department of Veterinary Biosciences, The Ohio State University, Columbus, Ohio 43210, and Department of Physics, Emory University, Atlanta, Georgia 30322

Received April 5, 2004; Revised Manuscript Received July 21, 2004

ABSTRACT: Prolactin, a lactogenic hormone, binds to two prolactin receptors sequentially, the first receptor binding at site 1 of the hormone followed by the second receptor binding at site 2. We have investigated the mechanism by which human prolactin (hPRL) binds the extracellular domain of the human prolactin receptor (hPRLbp) using surface plasmon resonance (SPR) technology. We have covalently coupled hPRL to the SPR chip surface via coupling chemistries that reside in and block either site 1 or site 2. Equilibrium binding experiments using saturating hPRLbp concentrations show that site 2 receptor binding is dependent on site 1 receptor occupancy. In contrast, site 1 binding is independent of site 2 occupancy. Thus, sites 1 and 2 are functionally coupled, site 1 binding inducing the functional organization of site 2. Site 2 of hPRL does not have a measurable binding affinity prior to hPRLbp binding at site 1. After site 1 receptor binding, site 2 affinity is increased to values approaching that of site 1. Corruption of either site 1 or site 2 by mutagenesis is consistent with a functional coupling of sites 1 and 2. Fluorescence resonance energy transfer (FRET) experiments indicate that receptor binding at site 1 induces a conformation change in the hormone. These data support an "induced-fit" model for prolactin receptor binding where binding of the first receptor to hPRL induces a conformation change in the hormone creating the second receptor-binding site.

The idea that two spatially separated ligand-binding sites on a macromolecule are "functionally linked" was first proposed over 50 years ago by Jeffries Wyman in an attempt to explain the allosteric mechanism of hemoglobin oxygenation (*1*,*2*). The idea of functional linkage was further refined by Koshland in 1958, who proposed an "induced-fit" theory, which states that substrate binding to an enzyme could elicit a conformation change resulting in spatial rearrangement of the catalytic site (*3*). There are now numerous studies that have demonstrated that conformation changes are induced by the presence or absence of allosteric modulators, regulating the ligand-binding properties of enzymes and other proteins (*4*−*6*).

Our interests have focused on understanding how receptor-binding sites on hormones communicate with each other to induce receptor binding and dimerization. Our primary model has been the human lactogenic hormones, growth hormone (hGH)[1] and prolactin (hPRL). Both hormones bind to the prolactin receptor with a 1:2 stoichiometry. Binding of the two receptors is believed to be sequential, the first receptor binding at the hormone surface called site 1 followed by the second receptor binding at site 2 (*7*−*10*). Dimerized receptors activate one or more chemical signaling pathways within target cells (reviewed in refs *11* and *12*). However, the detailed mechanics of prolactin-receptor binding are not known.

Several crystal structures are available for hGH in free (*13*) and receptor-bound (*14*−*19*) forms (PDB nos. 1BP3, 1HGU, 1A22, 1AXI, 1HUW, 1HWH, 1HWG, 3HHR). Comparison of the crystal structures of receptor-free hGH (PDB no. 1HGU) and hGH bound to the extracellular domain of one hPRL receptor (hPRLbp) (PDB no. 1BP3) shows a distinct conformation change in the hormone upon receptor binding. Using site-directed mutagenesis, we have previously demonstrated that in hGH there exists a series of contiguous hydrophobic residues distal to the receptor binding sites that transmit the observed conformation change across the hormone (*20*). These data suggest that the receptor binding sites in hGH and other lactogenic hormones may be functionally coupled.

Recently an NMR structure for hPRL has been published (PDB no. 1N9D; *21*) (Figure 1). The major features are similar to those of hGH and ovine placental lactogen (PDB no. 1F6F)(*22*). The lack of structures describing hPRL bound to its receptor limits our knowledge of the receptor binding-induced changes in the conformation of this ligand. One explanation proposed for the ordered binding of hormone and receptor is that site 1 has a higher affinity for the receptor as compared to site 2 (*10*). This suggests that in the absence of receptor binding at site 1, there should still be receptor

† This work supported by Grant R01-DK056117 from the National Institutes of Health.

* Corresponding author. Mailing address: The Ohio State University, 1925 Coffey Road, Columbus, OH 43210. Tel: (614) 292-9641. Fax: (614) 292-8763. E-mail: brooks.8@osu.edu.

‡ The Ohio State Biochemistry Program, The Ohio State University.

§ Department of Veterinary Biosciences, The Ohio State University.

⊥ Emory University.

[1] Abbreviations: hPRL, human prolactin; hGH, human growth hormone; hPRLbp, extracellular domain (residues 1−210) of the human prolactin receptor; SPR, surface plasmon resonance; RU, resonance units; HEPES, 4-(2-hydroxyethyl)-1-piperazineethanesulfonic acid; DTT, dithiothreitol; CPM, 7-diethylamino-3-(4′-maleimidylphenyl)-4-methylcoumarin.

10.1021/bi049333p CCC: $27.50
Published on Web 10/09/2004

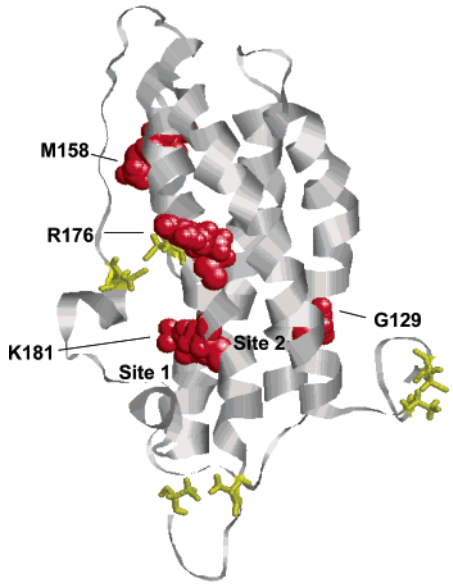

FIGURE 1: Ribbon diagram of the solution structure of hPRL (PDB no. 1N9D) (*21*). The residues mutated are shown in space fill (red). The six cysteine residues involved in disulfide bond formation are shown in yellow. The location of the two putative binding sites are indicated as site 1 and site 2.

binding at site 2. Studies of hGH binding to the somatotrophic receptor demonstrated that antibodies that block site 1 of hGH completely block receptor binding (*10*). This suggests that there may be another mechanism for sequential receptor binding.

We propose a model for hPRL receptor binding where, in the free hormone, site 2 is not structured for receptor binding. We believe that when the first receptor binds to site 1, the hormone undergoes a conformation change, similar to that observed in hGH, spatially reorganizing site 2 and allowing binding of the second receptor. We have used hPRL binding to the hPRLbp as a model to test our hypothesis.

We have chosen surface plasmon resonance (SPR) technology to determine the mechanism of hPRL receptor binding. This technology can be used to study equilibrium binding as well as the time-dependent interactions between molecules (*23*). One of the molecules (the ligand) is attached to a dextran-coated gold surface in a flow cell. The second molecule (the analyte) is then passed over this chip surface and an optical device on the opposite side of the gold surface detects the interaction between the two molecules based on changes in the refractive index within the flow cell. We utilized a unique approach to covalently attach hPRL to the chip surface using a specifically engineered cysteine that can be linked to the dextran polymer of the chip by formation of a disulfide bond (*24*). We mutated key residues in either site 1 (K181; *25*) or site 2 (G129; *8*) to cysteine. These residues were selected on the basis of structural (*18*, *21*) and functional homology (*8*, *25*). As a control, we mutated M158 to cysteine. This residue is distal to both the binding sites. When the hormone is covalently coupled to the chip surface through either K181C or G129C, the bulky dextran polymer blocks the respective binding site, allowing the receptor to bind to only one of the two sites. When M158C is bound to the chip, both sites are available for receptor binding. We used this approach to determine whether site 1 and site 2 binding occur independently or are functionally coupled.

EXPERIMENTAL PROCEDURES

Plasmids and Bacterial Strains. A hPRL DNA sequence for the mature methionyl protein was cloned into the pT7-7 derived phagemid (*26*) and was used for production of single-stranded DNA, site-directed mutagenesis, and expression of recombinant proteins in the *Escherichia coli* strains RZ1032 (*dut*$^-$, *ung*$^-$), DH5α, and BL21(DE3), respectively. Methionyl hPRLbp was also cloned into the pT7-7 phagemid and expressed in BL21(DE3) cells. The extracellular domain includes the first 210 amino acids of the mature hPRL receptor and was cloned from a human liver cDNA library (Invitrogen, Carlsbad, CA).

Site-Directed Mutagenesis. Site-directed mutagenesis was performed using the Kunkel method (*27*). Selection of positive clones was facilitated using translationally silent restriction sites that were introduced adjacent to the desired mutation. The desired mutations were confirmed using the Sanger dideoxynucleotide sequencing method (*28*).

Expression, Folding, and Purification of Proteins. Wild-type hPRL, the various hPRL mutants, and the hPRLbp were expressed in 1 L cultures of the BL21(DE3) strain of *E. coli* as previously described (*26*). The expressed proteins were collected as inclusion body pellets by centrifugation and were solubilized in 100 mL of 4.5 M urea, 100 mM Tris, pH 11.5. The pH was raised to reduce the stability of disulfide bonds. The proteins were refolded using extensive dialysis against 20 mM Tris, pH 7.5. The proteins were purified by anion-exchange chromatography using DEAE Sepharose Fast Flow (Amersham Biosciences, Piscataway, NJ) packed in a 20 mm × 100 mm column (Waters, Milford, MA). The purified proteins were dialyzed against 10 mM ammonium bicarbonate, lyophilized, and stored at −30 °C.

Characterization of Recombinant Proteins. The recombinant proteins were evaluated for size and purity using SDS-containing 15% polyacrylamide gel electrophoresis in the presence (reducing) or absence (nonreducing) of 2-mercaptoethanol. The molecular weights of proteins were measured on a Q-TOF II mass spectrometer (Micromass, Milford, MA). The correct folding of the proteins was determined by absorption, fluorescence, and circular dichroism spectroscopy at 20 °C in 20 mM Tris, pH 8.2, 150 mM NaCl. Protein concentrations were determined by the bicinchoninic acid assay (*29*).

Biological Assays. The biological activity of the recombinant hormones was determined in bioassays described previously (*20*). Briefly, serum-starved FDC-P1 cells stably transfected with the human prolactin receptor (*7*), a gift from Genentech, Inc. (San Francisco, CA), were plated in 96 well plates. The cells were then treated with varying hormone doses from 10 pM to 10 μM for 48 h. Hormone-induced cell proliferation was assessed using a vital dye method (Alamar Blue, Accumed International, West Lake, OH). Dose-response curves were used to determine the ED_{50} values for the recombinant wild-type and mutant hPRLs using a four-parameter fit (*30*).

The activity of hPRLbp was determined in a competition assay using FDC-P1 cells, where addition of hPRLbp sequestered hPRL and reduced hPRL-induced cell proliferation. hPRL (0.03 nM) was added to each of the wells along with increasing concentrations of hPRLbp from 0.01 nM to 10 μM. The effect of receptor-mediated sequestration of

hPRL on cell growth was determined by a vital dye as described above.

Immobilization of Hormones on the Dextran-Coated SPR Chip Surface. The optical biosensor was the BIAcore 3000 (Biacore Inc., Piscataway, NJ). The various hormone mutants were bound to the dextran surface of a CM5 sensor chip (BIAcore Inc.) using ligand-thiol coupling chemistry. The flow rate during ligand coupling was set at 5 μL/min. The chip surface was activated by injecting 10 μL of a mixture of 50 mM *N*-hydroxysuccinimide, 20 mM *N*-ethyl-*N*′-(dimethylaminopropyl)-carbodiimide. Disulfide groups were introduced on the activated chip surface by injecting 20 μL of 80 mM 2-(2-pyridinyldithio)-ethaneamine hydrochloride in 0.1 M sodium borate buffer, pH 8.5. The hormones, 200 nM in 10 mM sodium acetate buffer, pH 4.3, were coupled to the chip surface such that roughly 100 RU (resonance units, a measure of change in concentration of proteins on the sensor chip) of hormone was bound, corresponding to a ligand density of approximately 0.1 ng/mm^2 ($\sim$4 fmol/mm^2). The unreacted groups on the chip surface were subsequently blocked by 20 μL of 50 mM cysteine, 1 M NaCl, 0.1 M sodium formate buffer, pH 4.3. The buffer in hPRL/hPRLbp binding reactions was 10 mM HEPES, 150 mM NaCl, 3 mM EDTA, 0.005% Surfactant P20 (HBS-EP buffer).

Before the various mutants were bound to the CM5 sensor chip, they were treated with dithiothreitol (DTT) to reduce the free cysteine. The proteins in solution were incubated with a 5 μM excess of DTT for 5 min at room temperature. The DTT and proteins were then separated using a Microcon YM-10 centrifugal concentrator (Millipore Corporation, Bedford, MA). The centrifugation was repeated twice to ensure that >95% of the DTT was removed. Treated and untreated proteins were compared by UV spectroscopy to ensure that the DTT treatment did not affect endogenous disulfide bonds.

SPR kinetics between hPRL and hPRLbp may be limited by mass transport to the chip surface, artificially slowing the reactions. Two ways to minimize mass transport limitations are to increase the flow rate and to reduce the ligand concentration on the chip surface. Mass transport limitations were tested by flowing 50 nM hPRLbp across a chip with 100 RU of hormone at 5, 15, and 75 μL/min. The initial rates of binding were calculated. A variation of more than 10% in the initial rates is a sign that mass transport influences the kinetic data. Based on the results from this experiment, kinetics were not influenced by mass transport limits with a ligand concentration of 100 RU. The flow rate for the equilibrium and kinetic experiments was set at 50 μL/min.

Equilibrium Binding Experiments. For the equilibrium experiments, M158C, G129C, and K181C hPRLs were coupled to the CM5 sensor chip at various densities ranging from 100 to 1000 RU ($\sim$4 to 40 fmol/mm^2). A saturating concentration of hPRLbp (100 μM) was flowed over the chip surface at 50 μL/min to bind all available hormone binding sites irrespective of the receptor binding affinities. The binding stoichiometry of hPRLbp and hPRL was calculated at 200 s (after equilibrium was established) by normalizing the signals for their molecular weights with the formula:

$$\text{stoichiometric ratio} = \left(\frac{\text{RU of receptor}}{\text{RU of hormone}}\right)\left(\frac{\text{mol wt of hormone}}{\text{mol wt of receptor}}\right) \quad (1)$$

Binding of hPRLbp to the hPRL Mutants and Evaluation of Kinetics. Varying concentrations of hPRLbp from 50 to 800 nM were passed in a random order at 50 μL/min over a hormone-linked chip surface. The binding was recorded for 5 min. Dissociation of hormone and receptor was initiated by flowing buffer at 50 μL/min over the chip surface, and the signal was recorded for 5 min. Finally, the chip surface was regenerated to remove any remaining analyte by a 30 s injection of 2.5 M $MgCl_2$. The signal from each binding experiment was corrected for nonspecific binding by subtracting values obtained from a blank surface that had been activated and blocked with cysteine. In addition, the background-corrected receptor binding data were subsequently corrected for the signal produced from an injection of buffer across each ligand-linked chip surface. This double background correction has been recommended for analytical SPR studies (*31*). Based on the stoichiometric results of the equilibrium binding experiments, BIAevaluation 3.0 (BIAcore, Inc.) software was used to fit the kinetic data to models for 1:1 Langmuir binding for the mutant where site 2 was blocked (G129C hPRL), and based on the results of our saturation binding studies, a strictly ordered binding model (site 1 followed by site 2) was used when hPRL was coupled to the chip through M158C. The differential equations used for the strictly ordered binding model and the rationale for the equations used are described in Appendix 1. Association and dissociation rate constants were determined from these data. The equilibrium constants were calculated from the rate constants.

Fluorescence Resonance Energy Transfer. M158C hPRL was labeled with 7-diethylamino-3-(4′-maleimidylphenyl)-4-methylcoumarin (CPM, Molecular Probes, Eugene, OR, catalog no. D-346). The excitation and emission maxima for CPM are 358 and 469 nm, respectively. The hormone at 100 μM concentration was mixed with a 5-fold molar excess of CPM and incubated at room temperature with shaking for 4 h in 10 mM NH_4HCO_3, pH 7.0. The mixture was then passed through a Sephadex G50 column (Amersham Pharmacia) to separate the labeled hormone from the free fluorochrome. Mass spectrometry using the Q-TOF II spectrometer (Micromass, Milford, MA) verified that the hormone was labeled.

One micromolar labeled hormone was mixed with various concentrations of hPRLbp in 10 mM NH_4HCO_3, pH 7, as indicated in Figure 7. The samples were allowed to reach equilibrium at room temperature for 1 h. Fluorescence spectrum of each sample was collected by exciting the tryptophans at 295 nm and monitoring the emission spectra of CPM from 300 to 575 nm.

RESULTS

Purification and Spectroscopic Characterization of the Proteins. DNA sequencing confirmed that the plasmids encoded the desired proteins. SDS-containing 15% polyacrylamide gel electrophoresis of the proteins under reducing and nonreducing conditions (Figure 2) showed that the proteins were over 95% pure and ran at the predicted molecular weight. Nonreducing gels showed the formation of small amounts of dimeric proteins in some batches. These dimeric proteins were not observed under reducing conditions, indicating a disulfide linkage. Mass spectrometry was

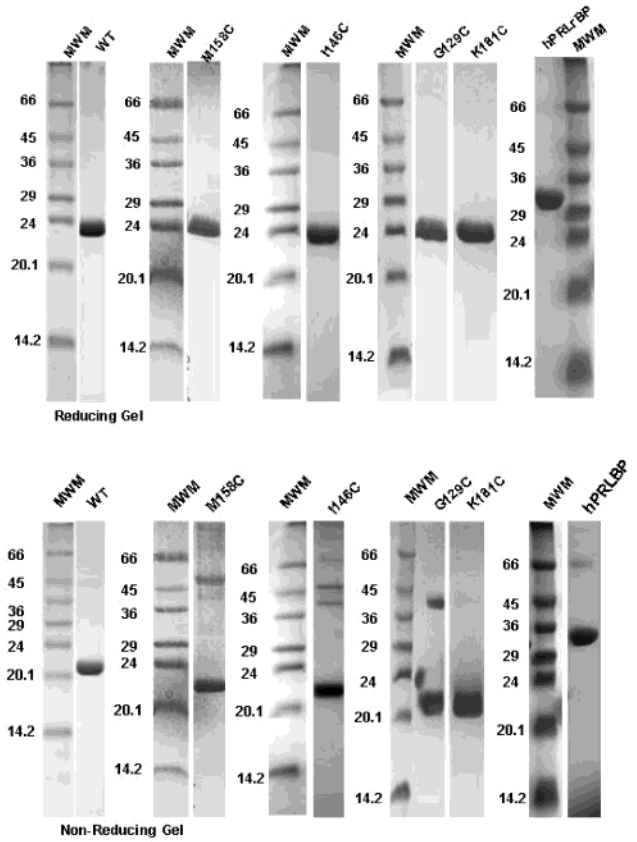

FIGURE 2: SDS-containing 15% polyacrylamide gel electrophoresis of recombinant proteins under reducing and nonreducing conditions. Gels are composites of results from typical batches of proteins. Each study was performed with a new batch of protein to include batch-to-batch variations in the preparation of proteins.

carried out to accurately determine the molecular weight of the various proteins (data not shown). The masses of the proteins were within 2 Da of their predicted values.

UV absorption spectra (Figure 3A) of all the mutants showed a peak around 277 nm, characteristic for the aromatic amino acids. Wild-type hPRL has a 280/250 nm absorbance ratio of approximately 2. The 250 nm absorption is largely due to disulfide bonds where absorbance is very sensitive to the stretching, bending, or turning of the disulfide bond. Thus, the 280/250 nm ratio is a sensitive indication of correct folding. All mutant or wild-type hPRLs used in these studies had a 280/250 nm absorption ratio between 1.8 and 2. Thus, correct disulfide bond formation was not affected by introduction of the seventh cysteine. No light scattering was observed at 350 nm indicating that the proteins did not form aggregates. Fluorescence spectra of the mutants overlap with wild-type hPRL with an emission maximum at 340 nm. Thus, the environment around the tryptophan and tyrosine residues was not disturbed by the free cysteine (Figure 2B). The variations in peak height of the fluorescence spectra can be attributed to variations in protein concentrations. CD spectra of wild-type hPRL and the mutants showed two negative peaks at 222 and 208 nm and a positive peak approaching 190 nm. This is characteristic for proteins that are predominantly α-helical (Figure 2C). Normalized peaks closely overlap (see inserts of Figure 2A−C), indicating that addition of the seventh cysteine at any of the three positions or other mutations failed to disturb the folded structure of the hPRLs. CD spectroscopy of hPRLbp indicated that the protein had

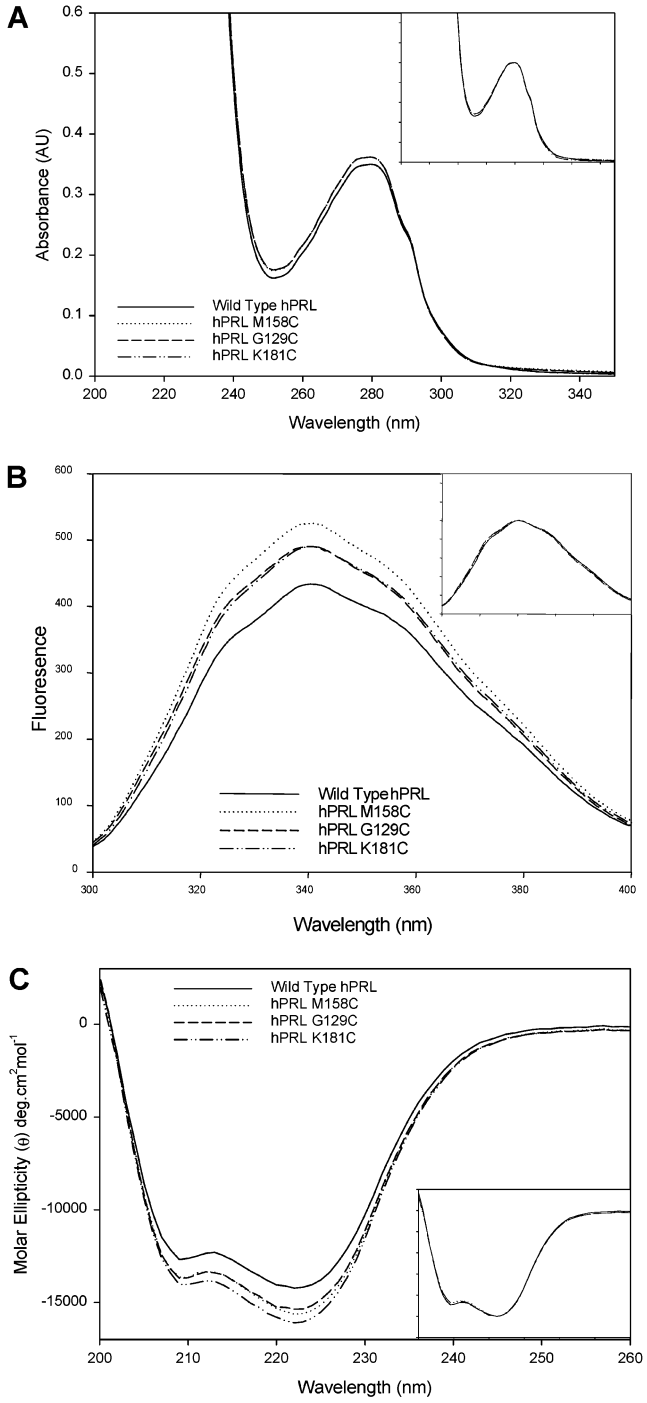

FIGURE 3: Spectroscopic characterization of the binding site cysteine mutants: (A) UV absorption at 25 μM protein concentration; (B) fluorescence spectroscopy at 1 μM protein concentration with 285 nm excitation; (C) circular dichroism spectroscopy at 25 μM protein concentration. The proteins were prepared in 10 mM Tris, pH 8.2, 150 mM NaCl. The inset contains data normalized to the wild-type hPRL peak maxima. All spectra were collected at 20 °C.

a β sheet structure with a negative peak at 215 nm (PDB no. 1BP3, data not shown) (*18*).

Biological Activity of the Cysteine Mutants. To determine whether the hPRL mutants were biologically active, we tested their ability to induce the proliferation of an FDC-P1 cell line stably transfected with the hPRL receptor. All mutant hPRLs were biologically active, although the activities of K181C and G129C were reduced. The ED_{50} values are

Table 1: ED_{50} Values of the Various hPRL Mutants

mutant	ED_{50} (nM)
wild-type hPRL	0.83
M158C	0.80
G129C	3.08
K181C	37.83
G129R/M158C	8.96
K181A/M158C	10.71
R176A/K181A/M158C	9.70

tabulated in Table 1. The loss of activity observed with G129C and K181C was expected since the mutations are directly in the receptor binding pockets of hPRL. The M158C mutation did not affect the biological activity of the hormone. Mutations in site 1 right-shifted the agonist and antagonist phase of the dose response curves. Mutations in site 2 (G129) reduced the maximal activity of the protein.

The biological activity of the hPRLbp was determined in a competition assay. The hPRLbp reduced the proliferative effect of hPRL in a dose-dependent manner on FDC-P1 cells transfected with the hPRL receptor, indicating that hPRLbp bound and sequestered hPRL (data not shown).

Equilibrium Binding Experiments with Site 1 or Site 2 Blocked. M158C, G129C, or K181C hPRLs were coupled to a CM5 sensor chip at various densities from 100 to 1000 RU. Five independent experiments were performed. A saturating concentration of the receptor (100 μM) was flowed across the chip surface, and the amount of receptor binding was determined (Figure 4A). Receptor binding to M158C, G129C, or K181C hPRLs approached equilibrium within a few seconds. M158C hPRL shows the maximum binding capacity, as expected since both binding sites are available. G129C hPRL (where site 2 is blocked) bound approximately 60% of the receptor that bound to M158C hPRL, while K181C hPRL (where site 1 is blocked) lost approximately 95% of the binding capacity when compared to M158C hPRL. This suggests that receptor binding at site 2 is dependent on prior receptor occupancy at site 1, but receptor binding at site 1 occurs regardless of receptor binding at site

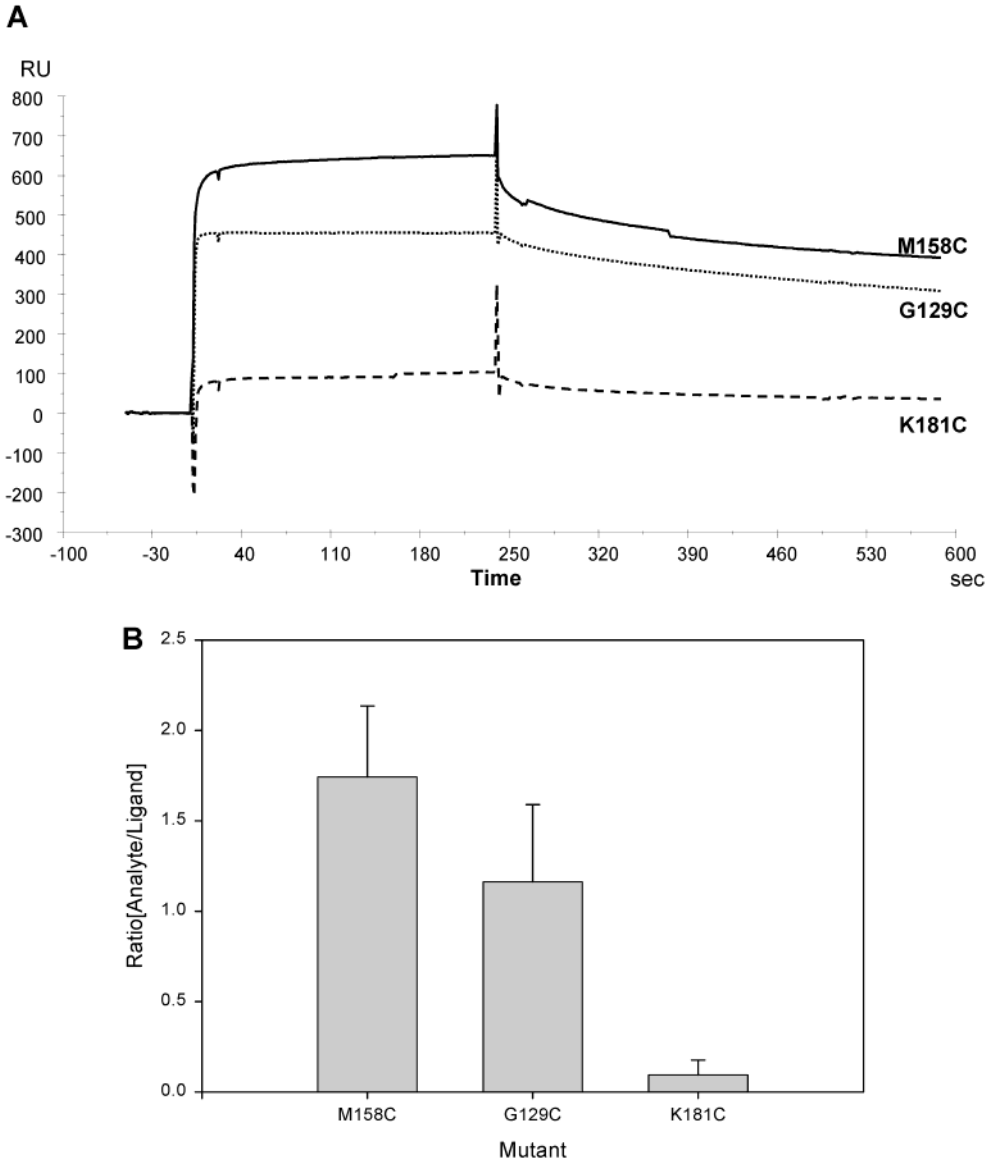

FIGURE 4: Equilibrium experiment using SPR. In panel A, 100 μM hPRLbp was passed over a CM5 sensor chip to which the hPRL cysteine mutants were coupled via disulfide bonds. A total of 300 RU of M158C hPRL, 300 RU of G129C hPRL, or 450 RU of K181C hPRL was coupled to the chip. hPRLbp association was followed for 4 min, and the dissociation was followed for another 4 min by running buffer over the chip surface. In panel B, the binding stoichiometry was calculated for five independent experiments.

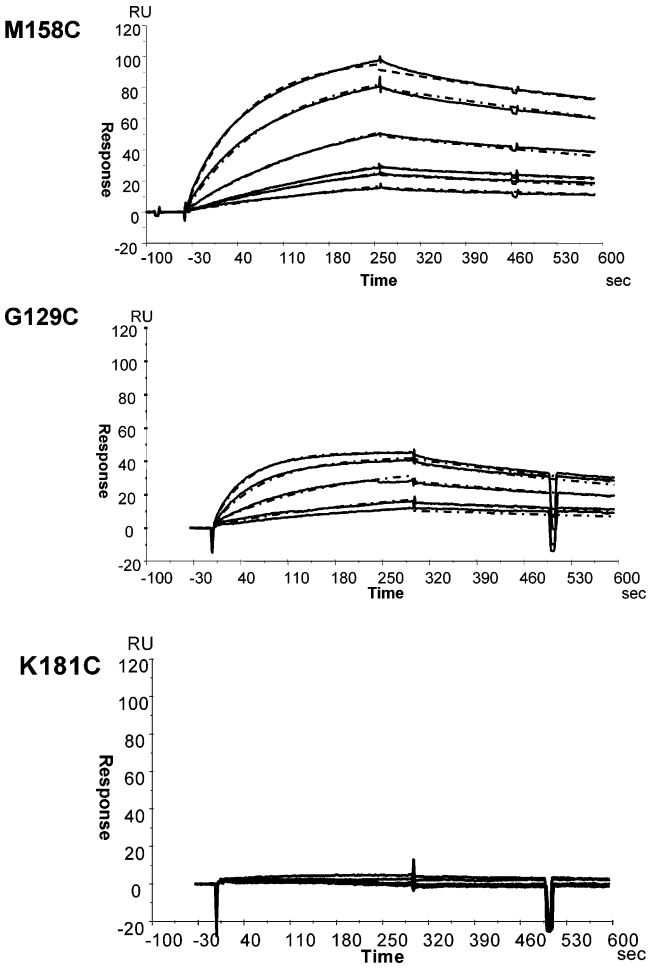

FIGURE 5: hPRLbp binding kinetics for the binding site cysteine mutants. The receptor (50, 80, 100, 200, 500, and 800 nM) was passed in random order over a CM5 chip to which about 100 RU of the various cysteine mutants was coupled. Association kinetics was followed for 5 min, and dissociation kinetics was followed for another 5 min by running buffer across the chip. The data for M158C hPRL (A) was fit to the two-site sequential-binding model and that for G129C hPRL (B) was fit to the 1:1 binding model. Data for K181C hPRL (C) could not be fit because the amount of bound hPRLbp was too low to accurately determine the kinetics. The solid lines (−) indicate the experimental data, and the dashed lines represent the binding curves predicted by the models.

2. If the two receptor binding sites in hPRL function independently, then at saturating receptor concentrations, both sites of wild-type hPRL should be occupied with receptor and the K181C mutant should have a similar receptor binding profile as G129C hPRL. This was not observed.

The average RU of receptor bound per RU of ligand attached was corrected for the relative molecular weights of the ligand and analyte, and the stoichiometric ratios of bound receptor per hPRL were calculated (Figure 4B) as in eq 1. The stoichiometries were 1.9 ± 0.4, 1.2 ± 0.4, and 0.1 ± 0.1 for M158C, G129C, and K181C hPRLs, respectively (mean ± SD). These stoichiometries suggest that two hPRLbps bind M158C hPRL, one hPRLbp binds G129C hPRL, and no hPRLbp binds to K181C hPRL.

Kinetics of Receptor Binding to M158C and G129C. The kinetic parameters for interactions between M158C or G129C hPRLs and hPRLbp were successfully determined (Figure 5, Table 2) using the models described in the Experimental Procedures and Appendix 1. The experiment was performed a minimum of three times. Various concentrations of hPRLbp (50, 80, 100, 200, 500, and 800 nM) were flowed at 50 μL/min in random order over a CM5 chip to which approximately 100 RU of M158C, G129C, or K181C hPRL was bound. The binding curves for M158C hPRL were fit to our strictly ordered binding model (equation 6A) and the curves for G129C hPRL were fit to the 1:1 Langmuir binding model. The binding curves from K181C hPRL could not be accurately fit since the amount of receptor bound was too low (less than 5 RU), providing binding information near the level of noise in our data. The χ^2 values for the fits were less than 5, indicating a good fit, and the residuals (a measure of the variance between the predicted model and the experimental data) were less than 4 RU. The experimental data for M158C and G129C hPRLs fit their respective models well. We also attempted to fit the data for M158C hPRL to a single-site model, but the fit was poor compared to that of the strictly ordered binding model (data not shown).

The association rate constants and dissociation rate constants for M158C and G129C hPRLs are presented in Table 2. The data are an average of at least three experiments. The equilibrium dissociation constant was derived from the average rate constants. Whether site 2 was blocked or not, the rate constants and derived equilibrium constants for site 1 did not significantly change when compared by a nonparametric *T*-test ($p > 0.05$) (compare k_{a1}, k_{d1}, and K_{D1} for M158C and G129C hPRLs, Table 2). Thus, binding of the receptor to site 1 was not greatly affected by the presence or absence of a functional site 2. In addition, the affinities at site 1 and site 2 appear to be similar (109 nM for site 1 compared to 153 nM for site 2). On the basis of the data presented, it appears that the differential affinity model does not describe the mechanism of hPRL/ hPRLbp interactions. The binding of hPRL and hPRLbp appears to be functionally coupled but atypically because site 1 binding influences site 2 but site 2 occupancy does not appear to influence site 1. The best description for this process is a strictly ordered binding process.

Receptor binding was also determined using another hPRL mutant, I146C. This mutation was a control to ensure that the results obtained with M158C were not an artifact of the mutation. When equal amounts of M158C or I146C were thiol-coupled to a sensor chip, they bound equal amounts of

Table 2: Rate and Equilibrium Constants for Receptor Binding to the Cysteine Mutants

	site 1			site 2		
mutant	k_{a1} (M^{-1} s^{-1}) ($\times 10^4$)	k_{d1} (s^{-1}) ($\times 10^{-3}$)	K_{D1} (nM)	k_{a2} (M^{-1} s^{-1}) ($\times 10^3$)	k_{d2} (s^{-1}) ($\times 10^{-4}$)	K_{D2} (nM)
M158C	1.42 ± 0.22	1.57 ± 0.37	109.42	2.56 ± 0.46	3.91 ± 3.86	153.11
G129C	1.96 ± 0.09	1.19 ± 0.11	60.54			
K181C[a]						

[a] Rate constants could not be calculated since the amount of receptor binding was too low.

receptor and showed identical binding profiles (data not shown).

Receptor Binding to hPRL Mutants with Increasing Disruption in site 1 or site 2. Since using dextran to completely disrupt site 1 or site 2 by the addition of a large molecule was rather drastic, several mutations that incrementally corrupt site 1 (K181A/M158C hPRL and R176A/K181A/M158C hPRL) or site 2 (G129R/M158C hPRL) by changing a few atoms were prepared and coupled to the CM5 chip through M158C. M158C hPRL was used as a control. The kinetic experiments were carried out as previously described for the cysteine mutants. The mutant hPRLs were folded correctly as determined by spectroscopic techniques (Figure 6A−C), but the biological activities were reduced approximately 10-fold (Table 1); reductions in biological activity are expected because the mutations will corrupt the topology of one of the receptor binding sites.

The binding of hPRLbp decreased as one and then two mutations were placed in site 1 (Figure 7A). In the case of K181A/M158C hPRL, the bound hPRLbp fell to approximately 30% of M158C hPRL. The double mutation (R176A/K181A) of site 1 reduced binding further to 20% binding as compared to M158C hPRL. In the case of site 2 corruption (G129R/M158C), binding to hPRL by 800 nM concentration of hPRLbp was approximately half of wild-type hPRL (Figure 7B).

Corruptions in site 1 reduced receptor binding between 70% and 80%. If the two receptor-binding events are independent, then the decrease should not be greater than 50% if the affinities for sites 1 and 2 are similar. Thus, our results indicate that binding at site 2 must be diminished along with site 1 binding. These results provide further support for the idea that receptor binding at site 1 is the critical step for binding at site 2 and formation of the trimeric hPRL−hPRLbp complex. The 50% decrease in receptor binding with the G129R hPRL was expected because alteration of site 2 reduces its affinity for hPRLbp but fails to influence the affinity of site 1 for hPRLbp. This study again indicates that site 1 binding is independent of site 2 binding.

Corruption of site 2 (G129R/M158C) did not significantly impact receptor affinity at site 1 (98.6 nM) compared to M158C hPRL (109.4 nM), again showing the inability of site 2 function to influence site 1. As expected, receptor-binding affinity at site 2 decreased about 10-fold in G129R hPRL, increasing the K_D from 153 to 1691 nM. The R176A/K181A corruption of site 1 decreased the receptor binding affinity at site 1 approximately 25-fold (2530 nM). The mutations in site 1 reduced the binding to such an extent that we could not reliably measure the affinity at site 2.

FRET Spectroscopy To Demonstrate Conformation Change. To determine whether hPRL (like hGH) undergoes a conformation change upon receptor binding at site 1, FRET spectroscopy was performed. We labeled M158C hPRL with a fluorochrome (CPM) via a maleimide coupling chemistry that displays a high propensity for reacting with free cysteine. This site is distal to the two hPRLbp binding sites in hPRL and would be the greatest distance from the tryptophans contained in hPRLbp binding at site 1 or 2. By placing the CPM at position 158, most of the signal would be generated by energy transfer from the two tryptophans in hPRL (W91 and W150). The downside of 158C-linkage is that position

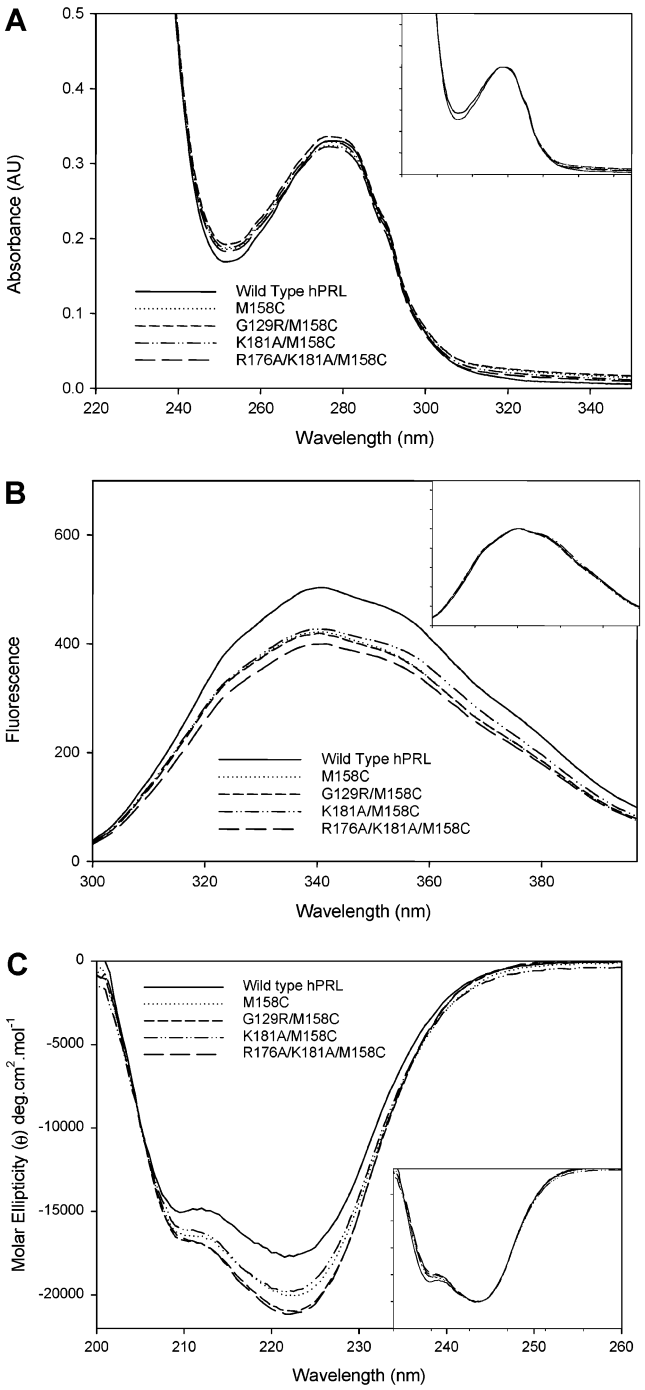

FIGURE 6: Spectroscopic characterization of the site 1 and site 2 mutants: (A) UV absorption at 25 μM protein concentration; (B) fluorescence spectroscopy at 1 μM protein concentration with 285 nm excitation; (C) circular dichroism spectroscopy at 25 μM protein concentration. The proteins were prepared in 10 mM Tris, pH 8.2, 150 mM NaCl. The inset contains data normalized to the wild-type peak maxima. All spectra were collected at 20 °C.

158 is not within site 2; thus a change in the FRET signal will indicate a conformation change in hPRL but may not address the situation in site 2. Alternatively, linking CPM in site 2 was considered. Placement here would bring CPM closer to the tryptophans in hPRLbp, mixing the signal from a conformation change with that for hPRLbp binding and proximity.

CPM labeling was verified by mass spectrometry, and approximately 25% of the protein was labeled. A peak with

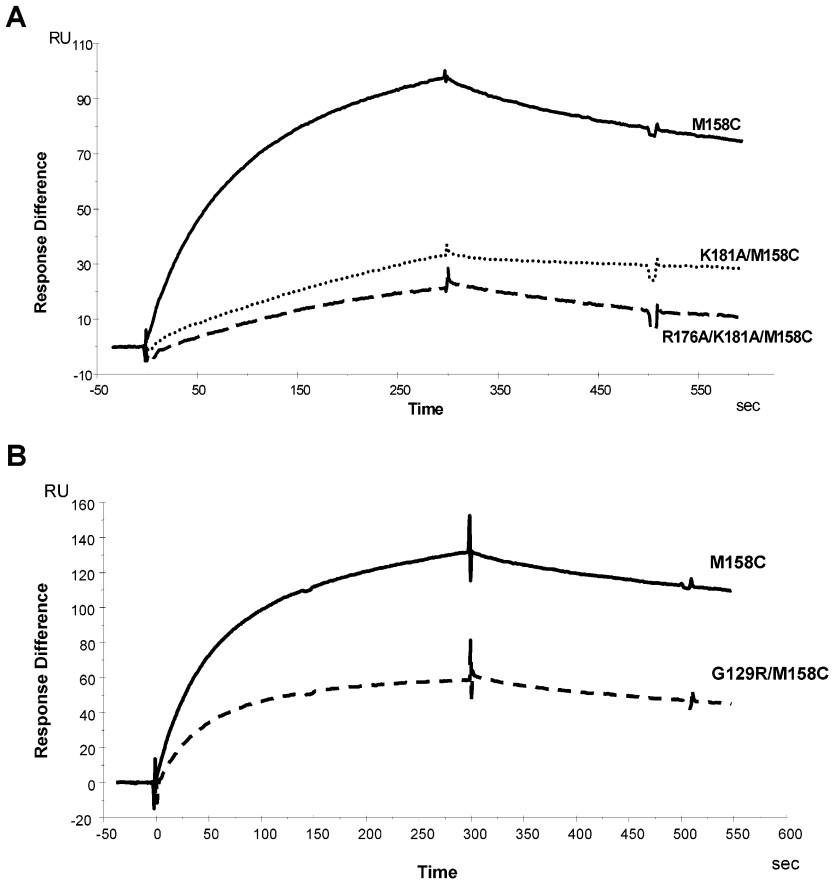

FIGURE 7: Binding profiles of the site 1 and site 2 mutants. hPRLbp (800 nM) was passed over a CM5 chip to which about 100 RU of the various mutants was coupled. Association kinetics was followed for 5 min, and dissociation kinetics was followed for another 5 min by running buffer across the chip.

a molecular weight corresponding to a single bound CPM was the predominant labeled form. A small peak corresponding to two bound CPM was also observed. The UV absorption spectra of labeled and unlabeled M158C hPRL were compared to verify that the tertiary structure of the protein was unaffected by the labeling process (data not shown). The unlabeled protein has a characteristic 280/250 nm UV adsorption ratio around 2. However this ratio is lowered to about 1 in the labeled protein due to an increased absorption at 250 nm. This suggests that the labeling has placed a strain on one or more of the disulfide bonds but failed to break the bond. If a disulfide bond had been broken, the absorbance at 250 nm would decrease and the 280/250 nm absorption ratio would have increased. On the basis of the mass spectrometry data indicating a small population of hPRL containing two CPM, it appears that only a small portion of protein may have a broken disulfide bond, and this might strain the remaining disulfide bonds on the double-labeled species. A portion of the labeled M158C hPRL then might have a broken disulfide bond and a CPM label at the reduced cysteine, thus making it unable to bind hPRLbp.

A 1 μM concentration of CPM-labeled M158C hPRL was incubated with increasing concentrations of hPRLbp that provided stoichiometric ratios between 0.5 and 2.5 for hPRLbp and total hPRL binding sites. The concentrations of hPRL and hPRLbp were within 10−50 times the apparent K_D; thus, increasing hPRLbp concentrations should produce FRET signals on the ascending portion of the binding isotherm. The reactions were allowed to approach equilibrium. The intrinsic tryptophan residues were selectively excited at 295 nm, and emission spectra were collected from 300 to 570 nm (Figure 8). The CPM emission maximum was approximately 469 nm, while the tryptophan emission maximum was approximately 340 nm. CPM fluorescence increased with hPRLbp concentrations. The distance-dependent increase in energy transfer from tryptophan residues to CPM suggested a hPRLbp binding-induced reduction in distance between the two fluorochromes.

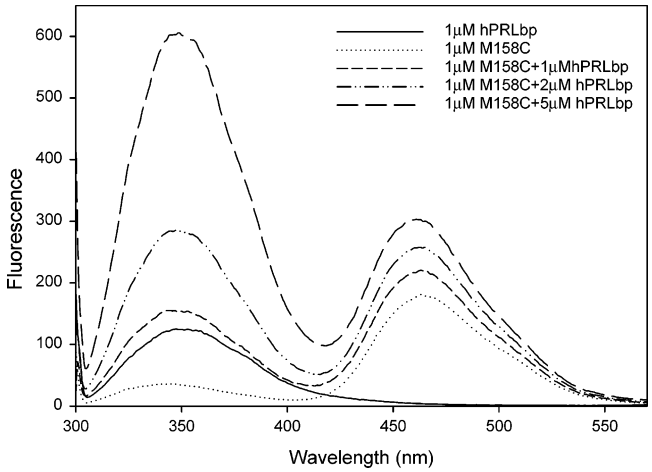

FIGURE 8: Fluorescence resonance energy transfer (FRET). CPM-labeled M158C hPRL (1 μM) was mixed with increasing receptor concentrations and allowed to come to equilibrium at 25 °C for 1 h in 10 mM NH_4HCO_3, pH 7.0. Samples were excited at 295 nm, and spectra were collected from 300 to 570 nm.

Table 3: Calculation of the Increase in FRET after Addition of Receptor to M158C hPRL

sample	cpm maximum intensity	area under the curve (420−550 nm)	difference
M158C	181.1	23 954	
M158C + 1 μM hPRLbp	220.5	29 687	5 773
M158C + 2 μM hPRLbp	257.8	35 163	11 209
M158C + 5 μM hPRLbp	302.8	42 202	18 248

An additional source of transferred energy could possibly come from the tryptophan residues in hPRLbp. We used the model of ovine placental lactogen bound to two rat prolactin receptors (*22*) to evaluate the distances between CPM and the tryptophans in either hormone or bound PRLbp. The sequences of hPRL/oPL and hPRLbp/rPRLbp were aligned to identify corresponding residues, and the relative positions of the corresponding residues were visually compared in the structures (PDB nos. 1F6F, 1BP3, and 1N9D) to confirm the appropriateness of the alignment. Rat and human PRLbp shared a 72% sequence homology and retained the topology of all tryptophans. oPL and hPRL shared a 45% sequence homology and retained the identical positions for their two tryptophans. Thus, we concluded that oPL/rPRLbp was an appropriate model for hPRL/hPRLbp. Distance measurements showed that the CPM label at residue 158 (corresponding to residue S160 in oPL) was approximately 14 and 27 Å from the nearest tryptophans in the hormone and rat PRLbp, respectively. Since the rate of energy transfer is inversely proportional to the sixth power of the distance, little energy is likely to be transferred from the tryptophans in hPRLbp. A similar distance (15 Å) was measured between the closest tryptophan and the α-carbon of hPRL, confirming the utility of the model. The increased fluorescence of CPM can thus be largely be attributed to an increased transfer of energy from the tryptophans in hPRL. The simplest explanation for this energy transfer is that there is a conformation change in the hormone upon receptor binding that brings the two fluorochromes closer together. The changes in fluorescence intensities are quantified in Table 3. The specificity of the signal was demonstrated by its quenching with a 50-fold excess of unlabeled hPRL (data not shown).

DISCUSSION

Using a novel approach to selectively block one or the other receptor binding sites in hPRL, we demonstrated a dependency of receptor binding at site 2 on occupancy of site 1 (Figures 4 and 5). In the absence of receptor at site 1, there was no occupancy or measurable affinity for the receptor at site 2 (Figure 5, Table 2). Once site 1 was occupied, there was a dramatic increase in site 2 affinity (Table 2). Incremental corruption of site 1 decreased the amount of receptor bound by greater than 50%, up to 80% with two site 1 mutations (Figure 7). These data showed that inhibition of binding at site 1 reduced the binding at site 2, because the inhibition was more than the 50% predicted if the sites were functionally independent. In contrast, mutating G129 to arginine in site 2 decreased the amount of receptor bound by approximately 50% (Figure 7), which would be expected if site 2 binding did not affect site 1. In addition, site 2 affinity in G129R hPRL decreased about 10-fold without a significant impact on site 1 affinity. Therefore, site 2 occupancy does not noticeably influence site 1 binding. These data support a strictly sequential binding mechanism for hPRL and hPRLbp. Binding studies of the hGH−hGHbp complex where site 2 was blocked using a monoclonal antibody showed that site 1 affinity is not altered by a blocked site 2 (*10*), suggesting a similar model for both hormones.

The FRET data supported the idea that a conformation change was the mechanism of communication between sites 1 and 2 (Figure 8). Our previous studies in hGH identified a hydrophobic motif that functionally coupled sites 1 and 2 (*20*). Site-directed mutagenesis also suggested that a similar motif might function in hPRL to couple sites 1 and 2 (Sivaprasad and Brooks, manuscript in preparation).

Sites 1 and 2 in hPRL were functionally coupled; thus a relationship of reciprocity may exist (Appendix, eq 5A) (*32*). Our data indicated that reciprocity was not observed because blocking site 2 did not significantly change site 1 affinity. M158C hPRL site 1 affinity was 109 nM, while G129C site 1 affinity was 60 nM; these values were not significantly different when the results of several experiments were compared. If reciprocity were present, then blocking site 1 would affect receptor binding at site 2, and blocking site 2 would affect binding at site 1. We observed coupled function in only one direction, site 1 binding activated site 2; thus, a different model than that in eq 5A needs to be invoked. Our data were consistent with a strictly ordered binding reaction (see Appendix).

$$H_{(00)} \underset{k_{1_{off}}}{\overset{k_{1_{on}}}{\leftrightarrow}} H_{(10)}R \underset{k_{2_{off}}}{\overset{k_{2_{on}}}{\leftrightarrow}} H_{(11)}RR \qquad (2)$$

In this mechanism, reciprocity was not apparent, and this strictly ordered model did not violate the first law of thermodynamics (the conservation of energy). We suggest that the energy derived from site 1 binding was partitioned with a portion paying for the conformation change of the hormone (and perhaps receptor) and the remainder lost as free energy. In the absence of site 1 bound receptor, site 2 binding was undetectable, and thus, the ability of site 2 binding to modulate site 1 affinity could not be tested.

Finally, the structure of the heterotrimeric hormone receptor complex complicates this model. Site 1 binding is thought to occur between distinct surfaces of hPRL and hPRLbp. The subsequent binding of the second hPRLbp to the dimeric complex uses two distinct binding surfaces; the first surface is between hPRL and hPRLbp, and the second surface is between the C-terminal domains of the two hPRLbp. In hGH/hGHbp binding the interface between the two hGHbps is responsible for generating a significant portion of the free energy of the second receptor interaction (*33*). The C-terminal interaction of the two receptors has yet to be measured for hPRLbps. But such an interaction will most probably affect the dissociation kinetics of the hPRLbp bound at site 1, thus being dependent on the binding status of the second receptor. In such a complex system, the reciprocal relationship between sites 1 and 2 demanded by functional coupling is obscured by the multisurface binding architecture.

ACKNOWLEDGMENT

We thank the application scientists from Biacore, Inc., for their helpful discussions. We would also like to thank Dr.

Kathleen Hayes for her help with the statistical analysis of the kinetic data. Dr. Karen Duda cloned the extracellular domain of the hPRL receptor, Jeffrey Basa prepared the M158C hPRL plasmid, and Piyanuj Patmastan prepared the I146C hPRL plasmid.

APPENDIX 1. DERIVATION OF AN ORDERED BINDING OF HUMAN PROLACTIN BINDING PROTEIN TO HUMAN PROLACTIN

The binding of hPRL to the hPRL receptor is a process that produces a heterotrimeric 1:2 hormone/receptor complex. The simplest model for formation of such a complex is where hPRL has two independent binding sites. When the independent binding site model is used, the reactions of hPRL and hPRLbp are

$$H_{(00)} + R \underset{k_{1_{off}}}{\overset{k_{1_{on}}}{\leftrightarrow}} H_{(10)}R \qquad \text{(receptor binding to site 1)} \tag{1A}$$

$$H_{(00)} + R \underset{k_{2_{off}}}{\overset{k_{2_{on}}}{\leftrightarrow}} H_{(01)}R \qquad \text{(receptor binding to site 2)} \tag{2A}$$

$$H_{(01)}R + R \underset{k_{1_{off}}}{\overset{k_{1_{on}}}{\leftrightarrow}} H_{(11)}RR \qquad \text{(receptor binding site 1)} \tag{3A}$$

$$H_{(10)}R + R \underset{k_{2_{off}}}{\overset{k_{2_{on}}}{\leftrightarrow}} H_{(11)}RR \qquad \text{(receptor binding site 2)} \tag{4A}$$

(Note that the numbers in parentheses represent the state of sites 1 and 2 on hPRL; the units place represents site 1, and the tens place represents site 2 with "0" indicating no bound receptor and "1" indicating a bound receptor).

If this model is correct then the order of receptor binding to hPRL can follow two pathways that can be summarized as follows:

$$\begin{array}{ccc} H_{(00)} & \leftrightarrow & H_{(10)}R \\ \updownarrow & & \updownarrow \\ H_{(01)}R & \leftrightarrow & H_{(11)}RR \end{array} \tag{5A}$$

In this model, binding is sequential but the order of binding is not specified, consistent with two independent binding sites.

Based on our SPR equilibrium experiments using saturating hPRLbp concentrations (Figure 3), we observed that site 2 does not bind hPRLbp unless site 1 has been bound first. In fact, the site 2 affinity in the absence of site 1 binding is not measurable with our SPR techniques. Therefore, $k_{2_{on}}$ is zero for reaction 2A. We assume that $H_{(01)}R$ is not produced by the dissociation of hPRLbp from site 1 of $H_{(11)}RR$. We make this assumption on the basis of the observation that hPRLbp dissociation is less likely to occur from the 2:1 complex because the hPRLbp bound at site 1 is also held to the complex by the attraction occurring between the two C-terminal domains of the hPRLbps. Bernat and colleagues have observed that much of the energy for formation of the trimeric complex between hGH and hGH bp comes from the interactions of the C-terminal domains of the receptor (*33*). Thus, $H_{(01)}R$ is unlikely to be produced by either the forward (reaction 2A) or reverse (reaction 4A) mechanisms. Consequently, the concentration of $H_{(01)}R$ will remain zero. Under these circumstances, the binding reactions simplify to

$$H_{(00)} \underset{k_{1_{off}}}{\overset{k_{1_{on}}}{\leftrightarrow}} H_{(10)}R \underset{k_{2_{off}}}{\overset{k_{2_{on}}}{\leftrightarrow}} H_{(11)}RR \tag{6A}$$

where *both* binding and dissociation are strictly ordered processes.

The differential equations for this ordered binding are

$$\frac{\partial[H_{(00)}]}{\partial T} = -k_{1_{on}}[H_{(00)}][R] + k_{1_{off}}[H_{(10)}R] \tag{7A}$$

$$\frac{\partial[H_{(10)}R]}{\partial T} = -k_{2_{on}}[H_{(10)}R][R] + k_{2_{off}}[H_{(11)}RR] + k_{1_{on}}[H_{(00)}][R] - k_{1_{off}}[H_{(10)}R] \tag{8A}$$

$$\frac{\partial[H_{(11)}RR]}{\partial T} = k_{2_{on}}[H_{(10)}R][R] - k_{2_{off}}[H_{(11)}RR] \tag{9A}$$

These equations were used to find the best-fit simultaneous solution for site 1 and site 2 binding using BiaEvaluation software 3.0.

Finally, on the basis of experiments where we demonstrated that the initial binding rates were not influenced by the flow rate of the hPRLbp solution, we concluded that binding at the chip surface was not influenced by depletion of the adjacent aqueous layer and the limits of analyte diffusion. On the basis of these findings, we have assumed that the analyte concentration throughout the system was identical to the concentration in the stock solution at any time during the binding experiments and that the free analyte concentration during the off rate studies was essentially zero. These assumptions are supported in our studies where binding hPRL to the chip surface at different densities did not systematically influence measured rates.

REFERENCES

1. Wyman, J. (1948) Heme proteins, *Adv. Protein Chem. 4*, 407−531.
2. Di Cera, E. (1998) Linkage Thermodynamics of macromolecular interactions, *Adv. Protein Chem. 51*, 59−120.
3. Koshland, D. E. (1958) Application of a theory of enzyme specificity to protein synthesis, *Proc. Natl. Acad. Sci. U.S.A. 44*, 98−104.
4. Mills, D. A., Seibold, S. A., Squier, T. C., and Richter, M. L. (1995) ADP binding induces long-distance structural changes in the.beta. polypeptide of the chloroplast ATP synthase, *Biochemistry 34*, 6100−6108.
5. Lee, J., Pilch, P. F., Shoelson, S. E., and Scarlata, S. F. (1997) Conformational changes of the insulin receptor upon insulin binding and activation as monitored by fluorescence spectroscopy, *Biochemistry 36*, 2701−2708.
6. Ghanouni, P., Steenhuis, J. J., Farrens, D. L., and Kobilka, B. K. (2001) Agonist-induced conformational changes in the G-protein-coupling domain of the beta 2 adrenergic receptor, *Proc. Natl. Acad. Sci. U.S.A. 98*, 5997−6002.
7. Fuh, G., Colosi, P., Wood, W. I., and Wells, J. A. (1993) Mechanism-based design of prolactin receptor antagonists, *J. Biol. Chem. 268*, 5376−5381.
8. Goffin, V., Struman, I., Mainfroid, V., Kinet, S., and Martial, J. (1994) Evidence for a second receptor binding site on human prolactin, *J. Biol. Chem. 269*, 32598−32606.

9. Goffin, V., Norman, M., and Martial, J. (1992) Alanine-scanning mutagenesis of human prolactin: importance of the 58−74 region for bioactivity, *Mol. Endocrinol. 6*, 1381−1392.
10. Gertler, A., Grosclaude, J., Strasburger, C. J., Nir, S., and Djiane, J. (1996) Real-time kinetic measurements of the interactions between lactogenic hormones and prolactin-receptor extracellular domains from several species support the model of hormone-induced transient receptor dimerization, *J. Biol. Chem. 271*, 24482−24491.
11. Argetsinger, L. S., Carter-Su, C. (1996) Mechanism of signaling by the growth hormone receptor, *Physiol. Rev. 76*, 1089−1107.
12. Bole-Feysot, C., Goffin, V., Edery, M., Binart, N., Kelly, P. A. (1998) Prolactin (PRL) and its receptor: actions, signal transduction pathways and phenotypes observed in PRL receptor knockout mice, *Endocr. Rev. 19*, 225−268.
13. Chantalat, L., Jones, N. D., Korber, F., Navaza, J., and Pavlovsky, A. G. (1995) The crystal structure of wild-type growth hormone at 2.5 Å resolution, *Protein Pept. Lett. 2*, 333−340.
14. Ultsch, M. H., Somers, W., Kossiakoff, A. A., and de Vos, A. M. (1994) The crystal structure of affinity-matured human growth hormone at 2 Å resolution, *J. Mol. Biol. 236*, 286−299.
15. Clackson, T., Ultsch, M. H., Wells, J. A., and de Vos, A. M. (1998) Structural and functional analysis of the 1:1 growth hormone: receptor complex reveals the molecular basis for receptor affinity, *J. Mol. Biol. 277*, 1111−1128.
16. de Vos, A. M., Ultsch, M., and Kossiakoff, A. A. (1992) Growth hormone and extracellular domain of its receptor: crystal structure of the complex, *Science 255*, 306−312.
17. Schiffer, C., Ultsch, M., Walsh, S, Somers, W., de Vos, A. M., and Kossiakoff, A. A. (2002) Structure of a phage display-derived variant of human growth hormone complexed to two copies of the extracellular domain of its receptor: evidence for strong structural coupling between receptor binding sites, *J. Mol. Biol. 316*, 277−289.
18. Somers, W., Ultsch, M., de Vos, A. M., and Kossiakoff, A. A. (1994) The X-ray structure of a growth hormone-prolactin receptor complex, *Nature 372*, 478−481.
19. Sundstrom, M. L. T., Rodin, J., Giebel, L. B., Milligan, D., and Norstedt, G. (1996) Crystal structure of an antagonist mutant of human growth hormone, G120R, in complex with its receptor at 2.9 Å resolution, *J. Biol. Chem. 271*, 32197−32203.
20. Duda, K. M., and Brooks, C. L. (2003) Identification of residues outside the two binding sites that are critical for activation of the lactogenic activity of human growth hormone, *J. Biol. Chem. 278*, 22734−22739.
21. Keeler, C., Dannies, P. S., and Hodsdon, M. E. (2003) The tertiary structure and backbone dynamics of human prolactin, *J. Mol. Biol. 328*, 1105−1121.
22. Elkins, P. A., Christinger, H. W., Sandowski, Y., Sakal, E., Gertler, A., de Vos, A. M., and Kossiakoff, A. A. (2000) Ternary complex between placental lactogen and the extracellular domain of the prolactin receptor, *Nat. Struct. Biol. 7*, 808−815.
23. Fagerstam, L. G., Frostell-Karlsson, A., Karlsson, R., Persson, B., and Ronnberg, I. (1992) Biospecific interaction analysis using surface plasmon resonance detection applied to kinetic, binding site and concentration analysis, *J. Chromatogr. 597*, 397−410.
24. *BIAapplications Handbook*, Biacore AB, Uppsala, Sweden, 1998.
25. Kinet, S., Goffin, V., Mainfroid, V., and Martial, J. A. (1996) Characterization of lactogen receptor-binding site 1of human prolactin, *J. Biol. Chem. 271*, 14353−14360.
26. Peterson, F. C., Anderson, P. J., Berliner, L. J., and Brooks, C. L. (1999) Expression, folding, and characterization of small proteins with increasing disulfide complexity by a pT7−7-derived phagemid, *Protein Expression Purif. 15*, 16−23.
27. Kunkel, T. A., Bebenek, K., and McClary, J. (1991) Efficient site-directed mutagenesis using uracil-containing DNA, *Methods Enzymol. 204*, 125−139.
28. Sanger, F., Nicklen, S., and Coulson, A. R. (1977) DNA sequencing with chain-terminating inhibitors, *Proc. Natl. Acad. Sci. U.S.A. 74*, 5463−5467.
29. Smith, P. K., Krohn, R. I., Hermanson, G. T., Mallia, A. K., Gartner, F. H., Provenzano, M. D., Fujimoto, E. K., Goeke, N. M., Olson, B. J., and Klenk, D. C. (1985) Measurement of protein using bicinchoninic acid, *Anal. Biochem. 150*, 76−85.
30. Munson, P. J., and Robard, D. (1980) Ligand: a versatile computerized approach for characterization of ligand-binding systems, *Anal. Biochem. 107*, 220−239.
31. Myszka, D. G. (1999) Improving biosensor analysis, *J. Mol. Recognit. 12*, 279−284.
32. Di Cera, E. (1998) Linkage thermodynamics of macromolecular interactions, *Adv. Protein Chem. 51*, 59−119.
33. Bernat, B., Pal, G., Sun, M., and Kossiakoff, A. A. (2003) Determination of the energetics governing the regulatory step in growth hormone-induced receptor homodimerization, *Proc. Natl. Acad. Sci. U.S.A. 100*, 952−957.

BI049333P